

# Produce of Biodegradable Porous Mg-Zn Scaffold via Powder Metallurgy and Coated with Nano HAP Synthesized by Electrodeposition Process

Z.S. Seyedraoufi<sup>1,\*</sup>, Sh. Mirdamadi<sup>1</sup>

<sup>1</sup>*School of Metallurgy and Materials Engineering, Iran University of Science and Technology, Tehran, Iran.*

*Received: 11 March 2017 - Accepted: 15 April 2017*

## Abstract

Mg is considered promising degradable material for tissue engineering applications because of good biocompatibility, corrosion and mechanical properties. In the present work, biodegradable porous Mg-1 wt% Zn scaffold was produced by powder metallurgical process and then nano hydroxyapatite (HAP) coating with composition of  $\text{Ca}_{10}(\text{PO}_4)_6(\text{OH})_2$  on the scaffold was synthesized by pulse electrodeposition and alkali treatment processes to increase the corrosion resistance of the substrate. The results showed that the as-deposited coating consists of HAP,  $\text{CaHPO}_4 \cdot 2\text{H}_2\text{O}$  (DCPD) and  $\text{Ca}_8\text{H}_2(\text{PO}_4)_6 \cdot 5\text{H}_2\text{O}$  (OCP) with plate-like and needle-like morphologies and the post-treated coating was composed of needle-like structure of nano HAP developed almost perpendicularly to the substrate. Electrochemical tests indicated that the corrosion current density reduced from  $2.731 \times 10^{-3}$  to  $4.98 \times 10^{-5}$   $\text{A} \cdot \text{cm}^{-2}$  and the corrosion potential of scaffold increased from -1.451 to -1.37 V. This study revealed that electrodeposition of HA coating is a useful approach to improve the corrosion resistance of porous Mg-Zn scaffold in SBF and to develop Mg-based degradable implants.

**Keywords:** Biodegradable Scaffold, Mg-Zn, HAP Coating, Electrodeposition, Corrosion Resistance.

## 1. Introduction

The development of a scaffold, a three-dimensional porous structure, is one of the most attractive subjects in tissue engineering that plays a key role in assisting tissue regeneration [1]. A scaffold must be bioactive, porous, and biodegradable and possess adequate mechanical properties suited to the biological site. To accommodate cell differentiation and proliferation, sufficient porosity is needed which will eventually enhance tissue formation [2]. A bioactive scaffold promotes cell-biomaterial interactions, cell proliferation, adhesion growth, migration, and differentiation.

A biodegradable scaffold allows the replacement of biological tissues through physiological extracellular components without leaving toxic degradation products. Its degradation rate should match the rate of new tissue regeneration in order to maintain the structural integrity and provide a smooth transition of the load transfer from the scaffold to the tissue [2]. Thus, as a mechanical support, a scaffold must possess adequate mechanical stability to withstand both the implantation procedure and the mechanical forces that are typically experienced at the scaffold-tissue interface and does not collapse during patient's normal activities. Achieving adequate initial strength and stiffness and maintaining them during the stage of healing or neo-tissues generation throughout the scaffold degradation process is the

major challenge [3-5].

Porous Mg scaffold plays a significant role in cell proliferation and growth. As Mg is found in bone tissue, it is an essential element to human body, and its presence is beneficial to bone growth and strength [6-9]. Owing to their good biocompatibility and rather low mechanical stiffness (i.e., low Young's modulus), Mg-alloys are potential candidates for biodegradable implants [10]. Exceedingly high corrosion rates of Mg alloys in physiological conditions make their biodegradability to be faster than the time required to healing the bone [10,11]. For this reason it is important to decrease the degradation rate of Mg alloys using different techniques such as alloying, purification and surface coating [11-13].

Mg is usually alloyed with other metals. Other elements alloying has been studied for developing biodegradable magnesium alloys with good corrosion and mechanical properties [13,14]. Zn is as the alloying element to get the good biocompatibility and Zn is necessary microelement and component of many proteins and nucleic acid of human body. Also Zn can increase the metabolism of cells. The addition of Zn to Mg to produce the Mg-Zn scaffold improves both the corrosion resistance and mechanical properties of magnesium alloys [15-18]. HAP is currently used as a biomedical material due to its excellent biocompatibility [19]. Nano HAP coating can match to the bone structure. Many processes have been created to synthesize of HA coating on the metallic substrates, such as sol-gel, biomimetic, electrophoretic deposition and sputtering processes;

\* Corresponding author

Email address: zahrasedraoufi@alumni.iust.ac.ir

but, because Mg and Mg alloys have low melting point, these methods cannot be used to deposit HAP coating [20]. Electrochemical deposition has unique advantages due to its capability of forming a uniform coating on a porous substrate or one with a complex shape, its controllability with regard to the thickness and chemical composition of the coating, and its low deposition temperature [19-22]. In the traditional electrodeposition process, loose, porous and low adhesive coatings develop. Thus, pulse electrodeposition method is suggested for deposition of an adherent coating [22-24]. In this present work, Porous Mg-1 wt.% Zn scaffold synthesized as substrate using a powder metallurgy method; then, HAP coating was deposited on the porous Mg-1 wt.% Zn scaffold using the pulse electrochemical deposition method and post-treated in alkali solution as HA is the most stable calcium phosphate ceramic in alkaline solution [21]. The compositional and microstructural changes of specimens after different treatments, as well as the degradation behavior of as-synthesized, as-deposited and post-treated porous Mg-1 wt. % Zn samples in simulated body fluid (SBF) were investigated.

## 2. Materials and Methods

Pure Mg (purity  $\geq 99\%$ , particle size  $\leq 100 \mu\text{m}$ ) and pure Zn (purity  $\geq 99.8\%$ , particle size  $\leq 45 \mu\text{m}$ ) powder were utilised as starting materials. Carbamide ( $\text{CO}(\text{NH}_2)_2$ ) particles were employed as the space-holder agent. The particle size of the spacer agent material was in the range of 200 to 400  $\mu\text{m}$  with a purity of 99.9%. After mixing the starting materials with the space-holder particles, porous Mg-1 wt. % Zn samples were prepared through a powder metallurgy process. The mixtures of Mg and Zn powder were prepared based on 1 wt. % Zn amount, while the carbamide particles were thoroughly added to the above specimens with volume content of 15%.

The mixed powder was uniaxial pressed at a pressure of 200 MPa into green compacts with dimensions of 10 mm in diameter and 13 mm in length. The green compacts were subsequently heat treated to burn out the spacer particles and sinter the porous Mg-Zn specimens separately in a tube furnace under an argon atmosphere. The heat treatment process was consisted of two steps: first heating up to 250°C at a rate of 3.75 degrees per minute and staying at that temperature for 4 h, and then heating up to 550°C at a rate of 8 degrees per minute and staying at the final temperature for 2 h. The synthesized Mg-1 wt. % Zn scaffold was considered as the substrate material. During the electrodeposition, an Mg-1 wt. % Zn alloy sample

was used as the working electrode and cylindrical graphite was served as the counter electrode. Before deposition, in order to obtain a clean and fresh working surface, the samples were sequentially polished with silicon carbide papers of 400–1000 grits, cleaned ultrasonically in acetone, activated with 10%  $\text{HNO}_3$  for 10 second, and dried using a drying apparatus. The electrolyte used for deposition of calcium phosphate was prepared by mixing a solution of 0.042 mol  $\text{L}^{-1}$   $\text{Ca}(\text{NO}_3)_2$ , 0.025 mol  $\text{L}^{-1}$   $\text{NH}_4\text{H}_2\text{PO}_4$  and 0.1 mol  $\text{L}^{-1}$   $\text{NaNO}_3$ . The pH value of the electrolyte was adjusted to 5.0 by dilute  $\text{HNO}_3$  and  $(\text{CH}_2\text{OH})_3\text{CNH}_2$ . These reagents were all analytic grade. Deposition was performed with fixed frequency (100 Hz) by pulse peak current densities of 40  $\text{mA cm}^{-2}$ , positive pulse duty cycle of 0.1 and temperature of 85 °C. The duty cycle ( $\gamma$ ) corresponds to the percentage of total time of a cycle and is given by Eq. (1) [18]:

$$\text{Duty cycle } (\gamma) = t_{\text{on}}/t_{\text{on}} + t_{\text{off}} \quad (1)$$

$t_{\text{on}}$  is time of applied pulse potential and  $t_{\text{off}}$  is time of no current/ potential. The positive plating time was 10 ms and the deposition process lasted for 0.5 h. When the specimens were coated with calcium phosphate, they were removed from the electrolyte solution, rinsed in distilled water and dried for about 4 h in air. Then the as-deposited samples were immersed in 0.25 mol  $\text{L}^{-1}$   $\text{NaOH}$  solution at 80 °C for 4 h, rinsed in distilled water and dried at 80 °C for 4 h.

Chemical composition of the specimens was performed by X-ray diffractometer (XRD: Philips, 1800PW, Netherlands) with  $\text{Cu K}\alpha$  radiation. Morphology and element composition of the samples was identified by scanning electron microscope (SEM: Tscan-Vega, China) equipped with energy dispersion spectroscopy facility. The potentiodynamic polarization curves were obtained using a potentiostat (Autolab, PGSTAT302N, Netherlands) at a constant voltage scan rate of 5  $\text{mv s}^{-1}$ . Experiments were carried out in SBF at 37°C. A three-electrode cell with the samples as the working electrodes was used for the electrochemical measurements. The reference electrode was an Ag-AgCl electrode and the counter electrode was made of platinum. The area of the working electrode exposed to the solution was 0.85  $\text{cm}^2$ . The concentration of each ion in the SBF has been listed in Table 1. [25]. Solution was buffered at pH of 7.4 using tris-hydroxymethyl aminomethane ( $(\text{HOCH}_2)_3\text{CNH}_2$ ) and HCl at 37°C. Each result was taken as the mean value of testing on five samples.

**Table 1. Ion concentration in SBF [25].**

Ions	Na <sup>+</sup>	K <sup>+</sup>	Mg <sup>2+</sup>	Ca <sup>2+</sup>	Cl <sup>-</sup>	HCO <sub>3</sub> <sup>-</sup>	HPO <sub>4</sub> <sup>2-</sup>	SO <sub>4</sub> <sup>2-</sup>
Concentration (mmol L <sup>-1</sup> )	142.0	5.0	1.5	2.5	147.8	4.2	1.0	0.5

### 3. Results and Discussions

In Fig. 1 and 2., the optical and SEM micrographs of porous Mg-1 wt. % Zn scaffold are shown where the porosity of the specimen is  $\approx 23$  vol. % using Ref. [26]. The black phases belong to porosity and bright phases correspond to matrix. Some pores were interconnected and the porous magnesium-zinc had an open-cell structure. However, there were isolated pores which were not interconnected and formed as a result of volume shrinkage of the powders during the sintering process. EDS analysis of point A (Fig. 2.) is shown in Fig. 3. As observed in the pattern, the sintered scaffold contains Mg and Zn elements.

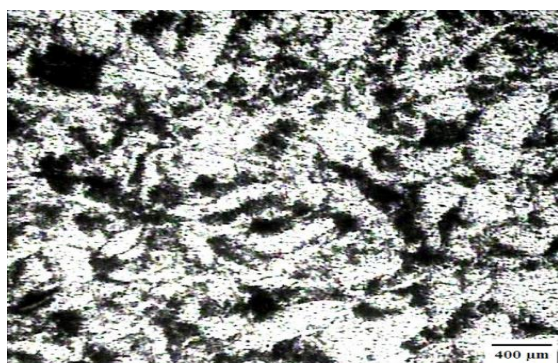


**Fig. 1. Optical micrograph of the Mg-1 wt. % Zn scaffold.**

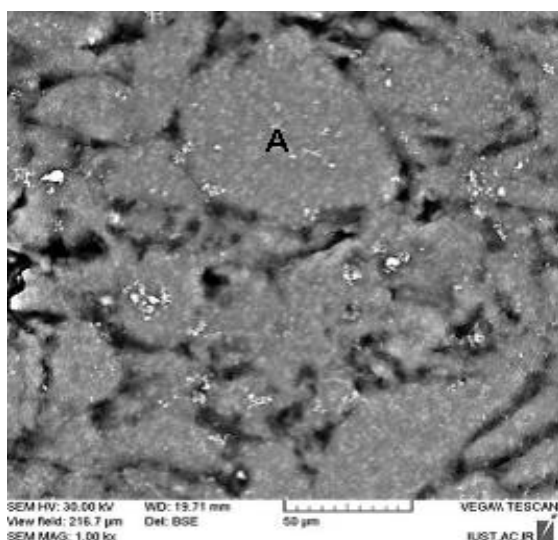


**Fig. 2. SEM micrograph of the Mg-1 wt. % Zn scaffold.**

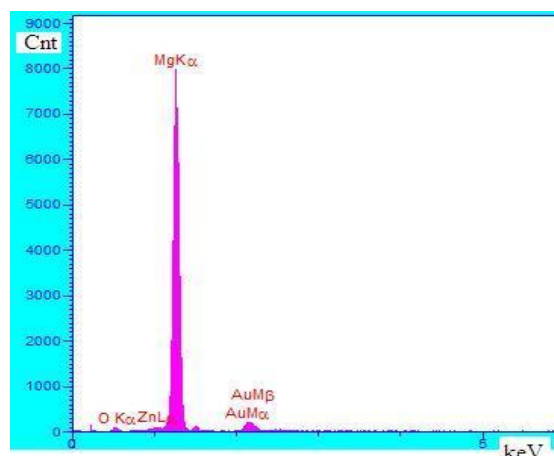


**Fig. 3. EDS analysis of the Mg-1 wt. % Zn scaffold.**

X-ray diffractometer (XRD) patterns of the as-deposited and post-treated coatings on porous Mg-1wt.% Zn scaffolds have been shown in Fig. 4. A mixture of HAP, DCPD and OCP was formed during electrodeposition process (as-deposited coating). In fact, with applying a high cathode current, the cathodic polarization of the Mg-Zn alloy leads to an increase in the pH at the interface between the alloy and the electrolyte. Not only does this increase in pH trigger crystal nucleation of the desired Ca-P phase directly on the scaffold surface, but also that initiates the Ca-P crystal growth. The electrodeposition reactions on the surface of scaffold are reduction reaction of  $\text{H}_2\text{PO}_4^-$  and  $\text{HPO}_4^{2-}$  and reaction of  $\text{Ca}^{2+}$  with  $\text{PO}_4^{3-}$ ,  $\text{OH}^-$  and  $\text{HPO}_4^{2-}$  to form HAP, DCPD and OCP. DCPD and OCP formed on the asdeposited coating are changed into HAP after alkali treatment with NaOH solution. SEM micrographs of the asdeposited and post-treated coatings have been shown in Fig. 5 and 6. The as-deposited and post-treated coatings have needle-like morphology less than 100nm in diameter. The as deposited coating shows some plate-like structures less than 100nm in thickness. This structure difference could be attributed to small amount of DCPD and OCP contained in the as-deposited coating. The needle-like structure might provide more area for the deposition of Ca and P in SBF compared to plate-like surface. In addition, in the post-treated coating, these needles are developed almost perpendicular to the substrate. It may be beneficial to have a needle-like structure for bone growth.

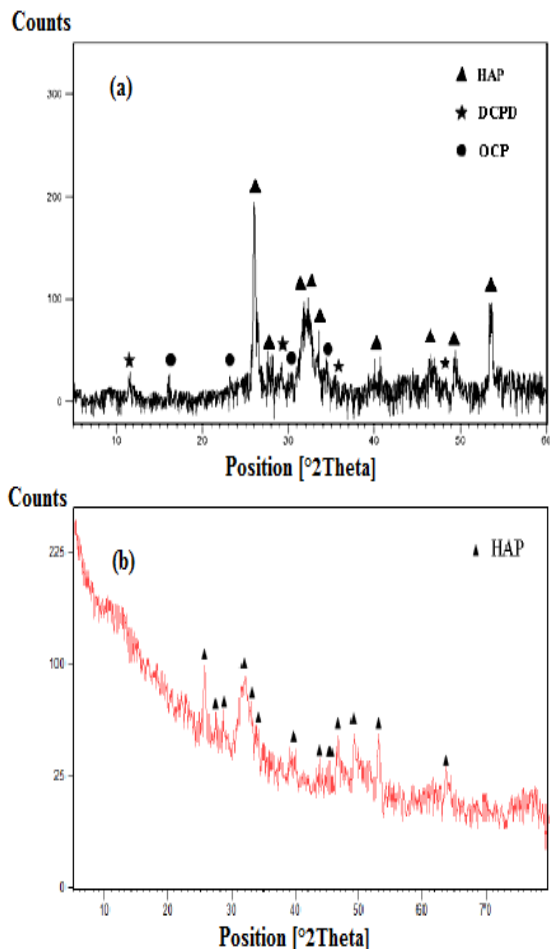


Fig. 4. XRD pattern of (a) as-deposited and (b) post-treated coatings.

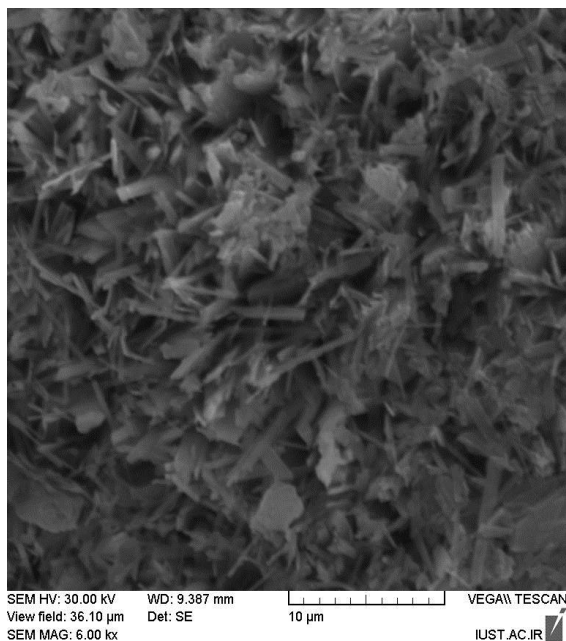


Fig. 5. SEM micrograph of as-deposited coating.

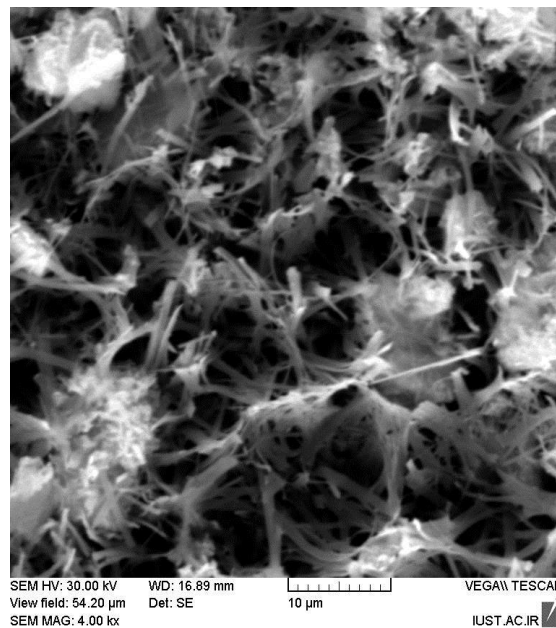


Fig. 6. SEM micrograph of post-treated coating by NaOH.

It is found that Ca/P atomic ratio is always improved to a certain extent after post-treating by NaOH due to DCPD and OCP having converted to HAP and may induce precipitation of a new bonelike apatite after. Thus, this just meets the requirements for biodegradable scaffolds [19].

Fig. 7. presents electrochemical polarization curves of different samples in SBF. The anodic polarization curves show a passivation-like region indicating the existence of a protective film on the surface of substrate. In fact, as Kannan and Raman [27] reported, phosphate and calcium ions in SBF could precipitate on the surface of Mg scaffold and, thus, a protective film will create on the surface of scaffold. In Table 2., Values of corrosion potential ( $E_{corr}$ ) and corrosion current density ( $i_{corr}$ ) are listed 1. The  $E_{corr}$  of scaffold significantly increased from -1.451 to -1.37 V after surface modification by HAP. According to the data,  $i_{corr}$  of Mg-1 wt. % Zn scaffold reduced from  $2.731 \times 10^{-3}$  to  $4.98 \times 10^{-5}$  A  $cm^{-2}$  which means HAP coating has increased the corrosion resistance of the scaffold in the SBF. In fact, the formed HAP coating protects scaffold from environmental attacks. It could be seen that  $E_{corr}$  and  $i_{corr}$  changed, respectively, from -1.39 to -1.37 V and from  $3.709 \times 10^{-4}$  to  $4.98 \times 10^{-5}$  A  $cm^{-2}$  after alkali treatment. Therefore, it is found that the alkali treatment can improve the Mg-Zn scaffold corrosion resistance. These phenomena indicate that the alkali treatment causes the HAP coating to have a better stability.

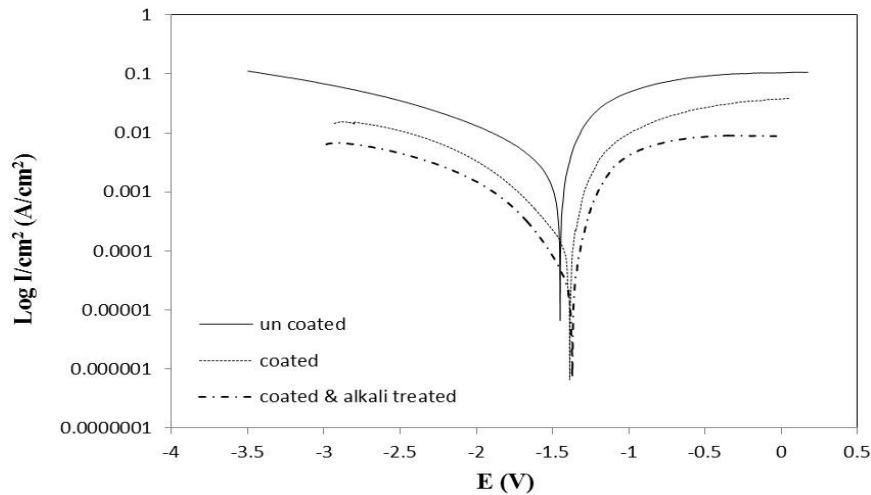


Fig. 7. Polarization curves of Mg-1 wt. % Zn scaffold, as deposited and post-treated HA-coated specimens in SBF.

Table 2. Electrochemical Parameters of the Scaffolds Obtained from the Polarization Curves.

Specimen	$E_{\text{corr}}$ (V)	$i_{\text{corr}}$ (A cm <sup>-2</sup> )
Mg-1 wt.% Zn scaffold	-1.451	$2.731 \times 10^{-3}$
As-deposited HAP-coated	-1.39	$3.709 \times 10^{-4}$
Post-treated HAP-coated	-1.37	$4.98 \times 10^{-5}$

#### 4. Conclusion

1. Biodegradable porous Mg-Zn Scaffold has been successfully produced via powder metallurgy process.
2. Nano hydroxyapatite coating with needle-like morphology was formed by pulse electrodeposition method to improve the biodegradation behavior of porous Mg-1 wt. % Zn scaffold.
3. The as-deposited coating containing calcium phosphates such as HAP, DCPD and OCP exhibited mainly needle-like and partially plate-like structures.
4. After alkali treatment, the post-treated coating showed needle-like HAP particles of less than 100nm in diameter.
5. The  $E_{\text{corr}}$  value of the Mg-1 wt.% Zn scaffold increased from -1.451 to -1.37 V and  $i_{\text{corr}}$  reduced from  $2.731 \times 10^{-3}$  to  $4.98 \times 10^{-5}$  A cm<sup>-2</sup> after scaffold surface modified by HAP coatings.

#### References

- [1] C.H. Chang, F.H. Lin, T.F. Kuo and H.C. Liu, *J. Biomed. Eng. Appl. Basis and Comun*, 17(2005), 1.
- [2] M.V. Risbud, M. Sittinger, *J. Trends in Biotech.*, 20(2000), 351.
- [3] J. Bonadio, E. Smiley, P. Patil and S. Goldstein, *J. Nat. Med.*, 5(1999), 753.
- [4] H.Y. Cheung, K.T. Lau, T.P. Lu and D. Hui, *J. Composites Part B.*, 38(2007), 29.
- [5] A.H. Yusop, A.A. Bakir, N.A. Shaharom, M.R. Abdul Kadir and H. Hermawan, *Int. J. Biomaterials*, 1(2012), 1.
- [6] N.E.L. Saris, E. Mervaala, H. Karppanen, J.A. Khawaja and A. Lewenstam, *J. Clinica. Chemica. ACTA*, 294(2000), 1.
- [7] J. Vormann, *J. Mol. Aspects Med.*, 24(2003), 27.
- [8] T. Okuma, *J. Nutr.*, 17(2001), 679.
- [9] M.P. Staiger, A.M. Pietak, J. Huadmai and G. Dias, *J. Biomaterials*, 27(2006), 1728.
- [10] F. Witte, V. Kaes, H. Haferkamp, E. Switzer, A. Meyer-Lindenberg, C. Wirth and H. Windhagen, *J. Biomaterials*, 26(2005), 3557.
- [11] Z.J. Li, X.N. Gu, S.Q. Lou and Y.F. Zheng, *J. Biomaterials*, 29(2008), 1329.
- [12] G.L. Song, *J. Corros. Sci.*, 49(2007), 1696.
- [13] S. González, E. Pellicera, J. Fornella and A. Blanquer, *J. Mech. behave. Bio-med. mater.*, 6(2012), 53.
- [14] Kh. Abdelrazek Khalil, *Int. J. Electrochem. Sci.*, 7(2012), 10698.
- [15] C.J. Deng, M.L. Wong, M.W. Ho, P. Yu and H.L. Dickon, *J. Composites Part A*, 36(2005), 551.
- [16] X. Gu, Y. Zheng, S. Zhong and T. Xi, *J. Biomaterials*, 31(2010), 1093.
- [17] A. Kaya, D. Eliezer, G. Ben-Hamu, O. Golan, Y.G. Na and K.S. Shin, *J. Met. Sci. Heat Treat.*, 48(2006), 50.
- [18] E. Zhang, D. Yin, L. Xu, L. Yang and K. Yang,

- Mater. Sci. Eng. C, 29(2009), 987.
- [19] H. Wang, S. Guan, X. Wang, C. Ren and L. Wang, *Acta Biomaterialia*, 6(2010), 1743.
- [20] M. Saremi, B. Motaghi Golshan, *Iranian J. Mater. Sci. Eng.*, 3(2006), 1.
- [21] Y. Song, D. Shan and E. Han, *Mater. Lett.*, 62(2008), 3276.
- [22] W. Li, S. Guan, J. Chen, J. Hu, S. Chen, L. Wang and S. Zhu, *Mater. Charac.*, 62(2011), 1158.
- [23] Z. Chun-Yan, Z. Rong-Chang, L. Cheng-Long and G. Jia-Cheng, *Surf. Coat. Technol.*, 204(2010), 3636.
- [24] E. Meng, S. Guan, H. Wang, L. Wang, S. Zhu, J. Hu, C. Ren, J. Gao and Y. Feng, *Appl. Sur. Sci.*, 257(2011), 4811.
- [25] T. Kokubo, H. Takadama, *J. Biomaterials*, 27(2006), 2907.
- [26] H. Zhuang, Y. Han and A. Feng, *Mater. Sci. Eng. C*, 28(2008), 1462.
- [27] M.B. Kannan, R. Raman, *J. Biomaterials*, 29(2008), 2306.